Ann. Geophys. Discuss., https://doi.org/10.5194/angeo-2018-9
Manuscript under review for journal Ann. Geophys.
Discussion started: 2 February 2018

Annales Geophysicae Discussions
Open Access
EGU

Statistical survey of day-side magnetospheric current flow using Cluster observations: Bow shock

Evelyn Liebert[1], Christian Nabert[1], and Karl-Heinz Glassmeier[1]

[1]Institut für Geophysik und extraterrestrische Physik, Technische Universtität Braunschweig

Correspondence: Evelyn Liebert (e.liebert@tu-bs.de)

Abstract. We present the first comprehensive statistical survey of the day-side terrestrial bow shock current system based on a large number of Cluster spacecraft bow shock crossings. Calculating the 3-D current densities using Fluxgate Magnetometer data and the Curlometer technique enables the investigation of current locations, directions and magnitudes in dependence on arbitrary IMF orientation. In case of quasi-perpendicular shock geometries we find that the current properties are in good accordance to theory and existing simulation results. However, currents at quasi-parallel shock geometries next to the foreshock region underlie distinct variations regarding their directions.

Keywords: Current systems (2708). Planetary bow shocks (2154). Instruments and techniques (2794).

1 Introduction

The terrestrial bow shock slows down the solar wind velocity to subsonic Mach numbers. This is accompanied by a gain in density, temperature and magnetic field strength. According to Ampère's law the bow shock carries electric currents which account for the jump in the magnetic field components tangential to the bow shock's surface. In contrast to the magnetopause, where the current directions are mainly determined by the geometry of the Earth's magnetic field, the direction of bow shock currents is solely determined by the orientation of the interplanetary magnetic field (IMF).

Depending on the local geometries of the shock surface and IMF orientation one distinguishes between quasi-perpendicular and quasi-parallel shocks where the IMF encounters the bow shock normal with angles above and below 45°, respectively. When encountering the compressed magnetic field at the shock some solar wind particles are reflected at the shock and re-accelerated in the solar wind's electric field while gyrating along the IMF direction before they enter the shock another time. At the quasi-parallel shock the reflected particles form the foreshock region where upstream waves are generated and alter the magnetic field configuration.

Until today, detailed bow shock current analysis based on in situ measurements has barely been done. Tang et al. (2012) presented a first statistical survey of bow shock currents using Cluster data from 25 crossing events when the IMF was dominated by its B_z component. They selected quasi-perpendicular shocks near the bow shock nose and calculated the current density from the magnetic gradient and the shock thickness. In this paper we extend the statistical survey of bow shock currents to overall 369 events covering both quasi-perpendicular and quasi-parallel situations during arbitrary IMF configurations for the first time. Making use of the simultaneously collected magnetic field data supplied by the multi-spacecraft mission Cluster

Ann. Geophys. Discuss., https://doi.org/10.5194/angeo-2018-9
Manuscript under review for journal Ann. Geophys.
Discussion started: 2 February 2018

Annales Geophysicae Discussions

(Escoubet et al., 2001) and applying the Curlometer technique (Dunlop et al., 1988) allows a direct 3-D investigation of the local current density vector.

2 Data selection and preparation

For our investigation we use Cluster magnetic field data from the Fluxgate Magnetometer (FGM) (Balogh et al., 2001) at spin resolution (0.25 Hz). Additionally, data from the Cluster Ion Spectrometry (CIS) instrument (Rème et al., 1997) are used to support the identification of bow shock crossings. The data are retrieved from the Cluster Active Archive (Laakso et al., 2010). Cluster consists of four individual spacecraft orbiting along a polar orbit with relative separations of a few kilometers up to over 10000 km. The thickness of the Earth's bow shock is about 100 to 1000 km. In order to match these spatial dimensions we use data obtained during periods when the average inter-spacecraft distance was small at the position of the bow shock. This criterion is fulfilled in the time range from February to May 2002 and from December 2003 to May 2004 when the average inter-spacecraft distance is about 300 km or less. At these times FGM and CIS data are available at the bow shock for 162 inbound and outbound orbit segments.

The Curlometer technique estimates the local current density across the Cluster tetrahedron volume by appoximating Ampère's law $\nabla \times \boldsymbol{B} = \mu_0 \boldsymbol{J}$. A thorough introduction to the Curlometer technique and an error analysis focussing on our application can be found in our previous publication (Liebert et al., 2017) where we conducted a similar study on magnetopause currents. The reliability of Curlometer results depends on the Cluster tetrahedron geometry which is constantly changing along its trajectory. One possibility to characterize the shape of the tetrahedron is given by the quality factor Q_G, which is defined by

$$Q_G = \frac{\text{True Volume}}{\text{Ideal Volume}} + \frac{\text{True Surface}}{\text{Ideal Surface}} + 1 \tag{1}$$

(e.g. Glassmeier et al., 2001), where the ideal volume and surface represent the volume and surface of a perfect regular tetrahedron with a side length equal to the average side length of the true tetrahedron. The quality factors equals one when the true tetrahedron is deformed into a linear geometry and three in case the true tetrahedron equals the ideal one. In this study we limit our investigation to bow shock crossings, where the quality factor takes values of 2.5 or more, leaving us 111 orbit segments. The usage of this quality factor for our investigation is discussed in detail by Liebert et al. (2017). $Q_G \geq 2.5$ allows us to expect accuracies of at least 2° to 10° in direction and 3 % to 15 % for the relative error in magnitude.

Dunlop et al. (2001) pointed out that high frequency fluctuations are likely to cause uncertainties within the Curlometer results and suggest an appropriate averaging in time before applying the Curlometer to magnetic field data. Regarding the bow shock crossing events examined in this study an averaging window of 30 s proved to be sufficient to damp highly fluctuating current signatures with spatial dimensions far below the tetrahedron size without altering current structures having dimensions of about 50 km and more along the spacecraft trajectory to a significant extent.

The bow shock transitions can be recognized easily within CIS particle data. At each transition event the edges of the corresponding current features are identified. We calculate the average current directions and magnitude for every event. Caused

Ann. Geophys. Discuss., https://doi.org/10.5194/angeo-2018-9
Manuscript under review for journal Ann. Geophys.
Discussion started: 2 February 2018

Annales Geophysicae Discussions
Open Access
EGU

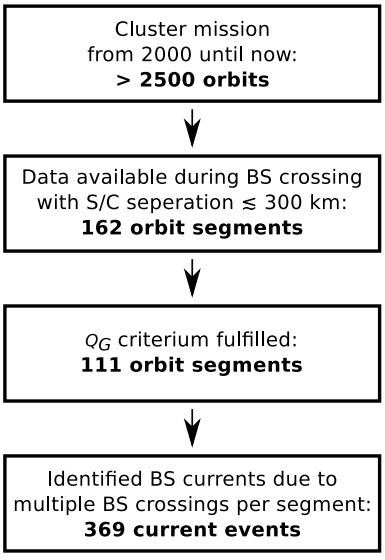

Figure 1. This sketch of the data selection process shows the shrinking amount of suitable data sets. From over 2500 Cluster orbits only a few orbit segments match the spatial requirements and the quality criterion for our bow shock current investigation.

by relative movement of the bow shock with respect to Cluster frequently multiple crossings are recorded within a short time along one orbit segment. This enlarges our data basis for the statistical survey to 369 current events (see Fig. 1).

3 Reference bow shock

The position and size of the bow shock vary depending on the solar wind conditions to a large extend. For representation of the bow shock crossing locations we introduce a parabolic model reference bow shock as a common frame of reference. Following Nabert et al. (2013) we use the the parametrization

$$x = \Delta_{\mathrm{BS}} - \sum_{t=y,z} c_{\mathrm{BS},t}\, t^2 \quad . \tag{2}$$

Δ_{BS} depicts the sub-solar bow shock stand-off distance with respect to the centre of the Earth (see Fig. 2). The geometric parameters $c_{\mathrm{BS},t}$ represent the bow shock curvature in $t = y$ and $t = z$ direction. Nabert et al. (2013) deduce values of

$$c_{\mathrm{BS},y} = 0.4\frac{1}{\Delta_{\mathrm{BS}}} \quad , \quad c_{\mathrm{BS},z} = 0.5\frac{1}{\Delta_{\mathrm{BS}}} \tag{3}$$

from an analytical zeroth-order approach solving the MHD-equations in the magnetosheath.

For each identified current the mean value of the tetrahedron barycentre's position vector is calculated. By radial projection along the Earth-spacecraft-line the intersection of this vector with the reference bow shock is calculated (cf. Fig. 2). The IMF is calculated by averaging the magnetic field data obtained during 5 minutes ahead of each bow shock current event. The

Ann. Geophys. Discuss., https://doi.org/10.5194/angeo-2018-9
Manuscript under review for journal Ann. Geophys.
Discussion started: 2 February 2018

Annales Geophysicae Discussions
Open Access
EGU

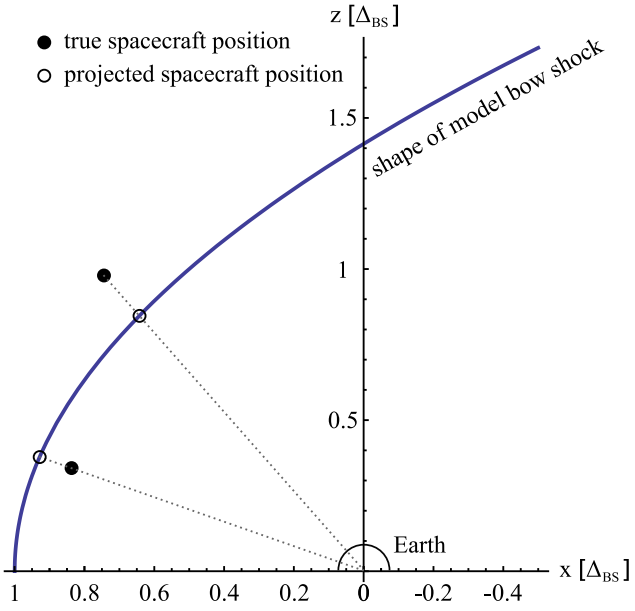

Figure 2. Sketch of the model bow shock used as a reference bow shock for data presentation. The dotted lines show example projections of two different currents from their true location to the location at the reference bow shock.

$\text{IMF}_{yz,GSE}$ component is used to define a new reference direction. For every event the GSE coordinate system is rotated around the x axis in such a way that the $\text{IMF}_{yz,GSE}$ component is orientated in positive z direction within the new system.

4 Results

4.1 Directions of bow shock currents

Depending on the angle Φ between local shock normal and IMF current events are categorized into quasi-perpendicular ($\Phi > 45°$) and quasi-parallel shocks ($\Phi < 45°$). The majority of 274 of the investigated currents represent quasi-perpendicular geometries. Fig. 3 shows the orientation of the current flow with respect to the model bow shock normal and the IMF. Most of the observed bow shock currents during quasi-perpendicular geometries lie nearly perpendicular to both the shock normal, which means that the currents flow parallel to the bow shock surface, and the IMF tangential component as it is expected from theory. The deviation from perpendicularity with respect to IMF_t is much larger in case of quasi-parallel shock situations (95 events) which reflects more turbulent and fluctuating conditions of the plasma flow adjacent to the foreshock region in contrast to the quasi-perpendicular shock. The broad distribution of the angle between current direction and reference bow shock normal indicates that the current flow direction at the quasi-parallel bow shock diverts extremely from the shape of a simplified bow shock surface.

Ann. Geophys. Discuss., https://doi.org/10.5194/angeo-2018-9
Manuscript under review for journal Ann. Geophys.
Discussion started: 2 February 2018

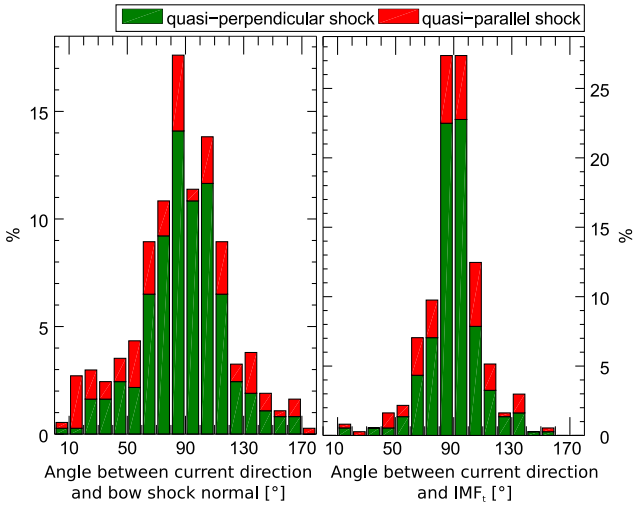

Figure 3. Orientation of current flow with respect to reference bow shock normal and IMF tangential component.

The global current direction distribution of the quasi-perpendicular and the quasi-parallel bow shock currents is displayed in Fig. 4 in the IMF-aligned coordinate systems. The current directions are represented by arrows of normalized length and the colour code indicates the direction of currents with respect to the x axis with red arrows pointing towards Earth and green arrows pointing towards sun. The current's flow direction is prescribed by the IMF orientation very clearly as they are collectively pointing along the positive y axis in the IMF-aligned coordinate system. The bottom panel of Fig. 4 displays histograms of the J_z direction with respect to the y axis including a sharp peak around 0° in the quasi-perpendicular case. In addition, the currents follow the draped shape of the bow shock pointing towards sun and Earth at the flanks. Again, more deviations are visible during quasi-parallel bow shock crossings (Fig. 4, right panels).

4.2 Current magnitudes

Figure 5 shows the occurrence distribution of investigated current magnitudes. The majority (about 80 %) does not exceed 30 nA m^{-2} and the values are in accordance to former single event results (e.g. Tang et al., 2012). The average current magnitude of all events is 19.4 nA m^{-2}.

MHD simulations (e.g. Lopez et al., 2011) predict a relatively broad region around the bow shock nose where the current magnitudes are constantly high. A weakening sets in at the high latitude bow shock. Investigating the spatial dependence of the event's current magnitudes results in a homogeneous distribution in case of the quasi-parallel shock events which all allocate at low latitudes (cf. Fig. 4). In case of quasi-perpendicular events current magnitudes near the bow shock nose are slightly larger than those at the flanks. The average magnitude of all quasi-perpendicular currents below 60° latitude is 22.3 nA m^{-2} while the average value of currents at higher latitudes is 16.1 nA m^{-2}.

The IMF magnitude is another controller of the bow shock current magnitude. Tang et al. (2012) found a linear relation between bow shock current and IMF$_z$ component at quasi-perpendicular bow shock events during north-ward and south-ward

Ann. Geophys. Discuss., https://doi.org/10.5194/angeo-2018-9
Manuscript under review for journal Ann. Geophys.
Discussion started: 2 February 2018

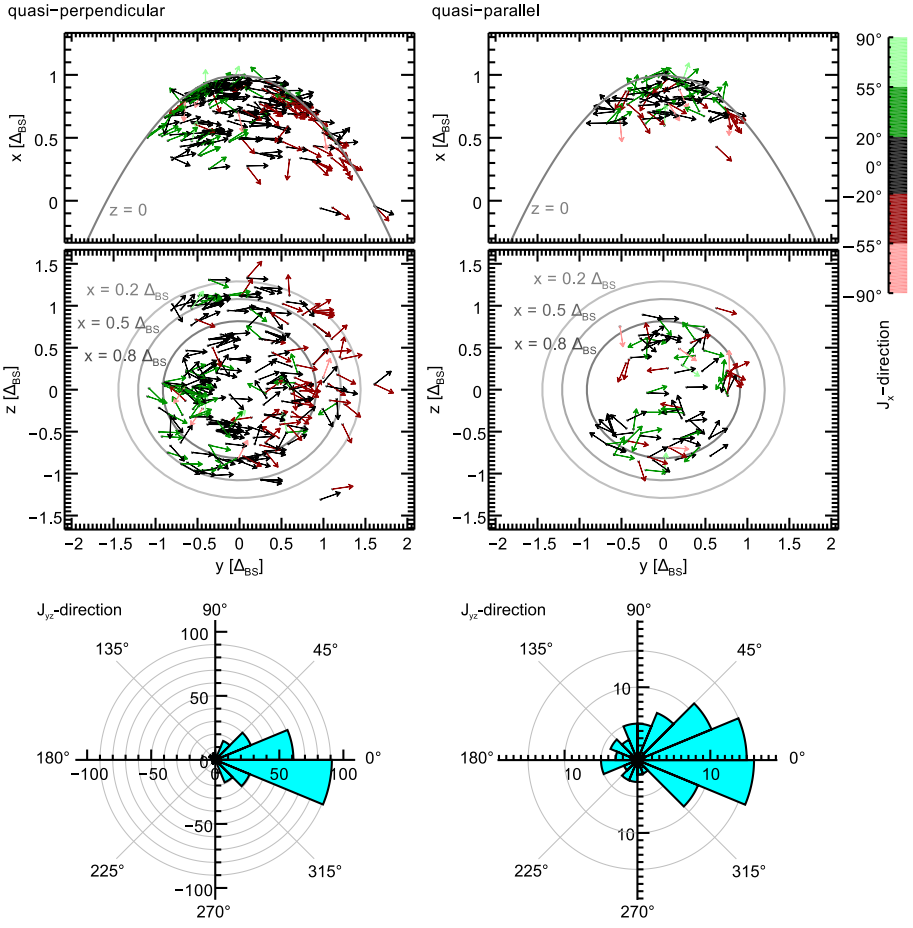

Figure 4. Bow shock current directions in *x*-*y* plane (top panel) and *y*-*z* plane (middle panel). J_x direction is represented by the colour code. The z axis of the coordinate system is aligned to the IMF_{yz} component. The grey paraboloid and ellipsoids represent the bow shock position at $z = 0$ and $x = 0.2, 0.5$ and $0.8\Delta_{\mathrm{BS}}$, respectively. Polar histograms (bottom panel) show the occurrence rates of current angles within in the *y*-*z* plane with respect to the positive *y* axis.

orientated IMF. Our survey shows that this correlation also applies to arbitrary IMF orientation and shock geometry. Figure 6 displays the average current magnitudes that are calculated for 1 nT intervals of the IMF component tangential to the bow shock surface. For quais-perpendicular and quasi-parallel cases magnetic field values up to 15 nT and 8 nT are observed, respectively. Within the range from 0 to 8 nT there are no distinct qualitative differences between quasi-perpendicular and quasi-parallel situations visible.

Ann. Geophys. Discuss., https://doi.org/10.5194/angeo-2018-9
Manuscript under review for journal Ann. Geophys.
Discussion started: 2 February 2018

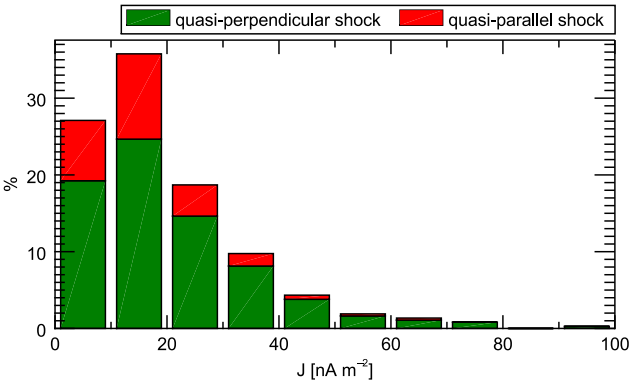

Figure 5. Occurrence rate of bow shock current magnitudes.

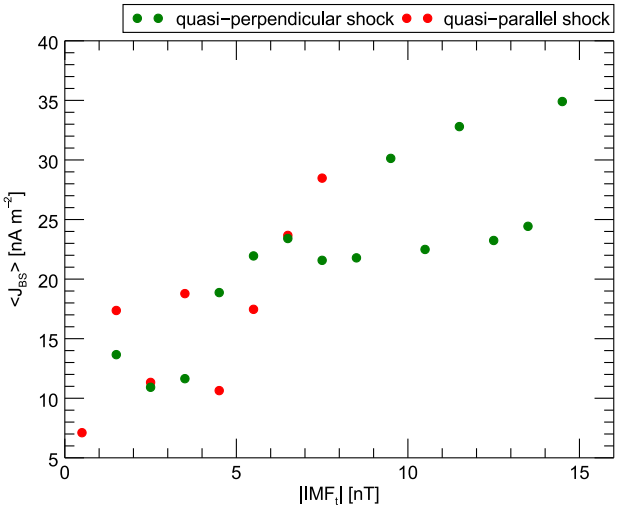

Figure 6. Current magnitude in dependence of the IMF tangential component. The IMF_t is binned into intervals of 1 nT. The current magnitude $<J_{BS}>$ is calculated by averaging over all current events that are ascribed to the corresponding interval.

5 Conclusions

The usage of the Curlometer technique allows us a direct investigation of 369 current events recorded within the magnetic field data obtained by Cluster during 111 bow shock crossings in 2002, 2003 and 2004. In 274 cases the bow shock represented a quasi-perpendicular shock ($\Phi > 45°$). In 95 events a quasi-parallel ($\Phi < 45°$) shock was observed. It lies adjacent to the foreshock region where solar wind particles are reflected back into the solar wind along the IMF direction and cause upstream and downstream perturbations of the magnetic field configuration.

At quasi-perpendicular shocks the bow shock currents are very clearly prescribed by the IMF direction fulfilling the equation $\nabla \times \boldsymbol{B} = \mu_0 \boldsymbol{J}$. The angle distribution between the bow shock current and IMF_t shows a sharp peak at $90°$. When displayed in

Ann. Geophys. Discuss., https://doi.org/10.5194/angeo-2018-9
Manuscript under review for journal Ann. Geophys.
Discussion started: 2 February 2018

Annales Geophysicae Discussions

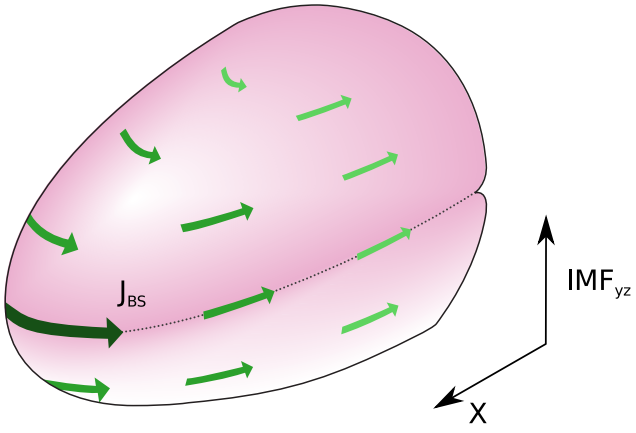

Figure 7. 3-D scheme of day-side bow sock shock current geometry and magnitude at the quasi-perpendicular bow shock. The greater and darker arrows represent higher values of current magnitude.

an IMF_{yz} aligned coordinate system the current directions arrows arrange themselves parallel to each other in the *y*-*z* plane. As the currents flow parallel to the shock surface, the draped shape of the bow shock becomes visible within the current direction in the *x*-*y* plane. The angle distribution between current and normal of the reference bow shock peaks at $90°$ as well but it is broadened to some extend as the reference bow shock naturally deviates from the true bow shock geometry.

The magnitudes of currents at the quasi-perpendicular bow shock generally increase with increasing tangential component of the IMF. Additionally, the current magnitudes are larger near the bow shock nose. Figure 7 is a schematic summary of our results for the currents observed at the quasi-perpendicular bow shock.

Typical values of the averaged current magnitudes obtained by the Curlometer technique are in the range of 5 to 40 nA m^{-2} with an average of about 20 nA m^{-2}. Those results are in accordance to former studies that calculated the current density via the jump in the magnetic field and a derived current sheet thickness.

The quasi-parallel shocks that we have found are all located at relatively low latitudes. In this region, we were not able to observe a spatial dependence of the current magnitude. Additionally, the IMF tangential component posses lower values only up to 8 nT. In this range we find that the dependence on the IMF magnitude seems to be qualitatively equal to that observed for quasi-perpendicular situations. In particular the current magnitudes of the quasi-perpendicular and the quasi-parallel bow shock are of similar size for a given IMF which is an interesting finding as the ideally (in reality never realized) parallel-shock would be accompanied by no jump in the magnetic field and therefore no current at all (Narita, 2006).

The direction of currents of the quasi-parallel bow shock are less prescribed by the IMF orientation compared to the quasi-perpendicular shock. Overall, the main characteristics are maintained but there are much more and larger deviations visible. In addition, the currents no longer lie perpendicular to the normal direction of the reference bow shock which indicates that the simplified model bow shock geometry does not hold at the quasi-parallel bow shock.

Ann. Geophys. Discuss., https://doi.org/10.5194/angeo-2018-9
Manuscript under review for journal Ann. Geophys.
Discussion started: 2 February 2018

Annales Geophysicae Discussions

Data availability. All Cluster data used in this study can be retrieved from the Cluster Active Archive.

Competing interests. The authors declare that they have no conflict of interest.

Acknowledgements. This work was financially supported by the German Ministerium für Wirtschaf und Energie and the Deutsches Zentrum für Luft- und Raumfahrt under contract 50OC1402. The author thanks the Cluster FGM and CIS Teams and the Cluster Science Archive for processing and providing the Cluster data.

Ann. Geophys. Discuss., https://doi.org/10.5194/angeo-2018-9
Manuscript under review for journal Ann. Geophys.
Discussion started: 2 February 2018

Annales Geophysicae Discussions

References

Balogh, A., Carr, C. M., Acuña, M. H., Dunlop, M. W., Beek, T. J., Brown, P., Fornaçon, K.-H., Georgescu, E., Glassmeier, K.-H., Harris, J., Musmann, G., Oddy, T., and Schwingenschuh, K.: The Cluster Magnetic Field Investigation: overview of in-flight performance and initial results, Annales Geophysicae, 19, 1207–1217, https://doi.org/10.5194/angeo-19-1207-2001, 2001.

Dunlop, M. W., Southwood, D. J., Glassmeier, K.-H., and Neubauer, F. M.: Analysis of multipoint magnetometer data, Advances in Space Research, 8, 273–277, https://doi.org/10.1016/0273-1177(88)90141-X, 1988.

Dunlop, M. W., Balogh, A., and Glassmeier, K.-H.: First Application of Multi-Point Magnetic Field Analysis Techniques: the Curlometer and the Discontinuity Analyser, in: Sheffield Space Plasma Meeting: Multipoint Measurements versus Theory, edited by Warmbein, B., vol. 492 of *ESA Special Publication*, p. 3, 2001.

Escoubet, C. P., Fehringer, M., and Goldstein, M.: Introduction The Cluster mission, Annales Geophysicae, 19, 1197–1200, https://doi.org/10.5194/angeo-19-1197-2001, 2001.

Glassmeier, K.-H., Motschmann, U., Dunlop, M., Balogh, A., Acuña, M. H., Carr, C., Musmann, G., Fornaçon, K.-H., Schweda, K., Vogt, J., Georgescu, E., and Buchert, S.: Cluster as a wave telescope â€“ first results from the fluxgate magnetometer, Annales Geophysicae, 19, 1439–1447, https://doi.org/10.5194/angeo-19-1439-2001, https://www.ann-geophys.net/19/1439/2001/, 2001.

Laakso, H., Perry, C., McCaffrey, S., Herment, D., Allen, A. J., Harvey, C. C., Escoubet, C. P., Gruenberger, C., Taylor, M. G. G. T., and Turner, R.: Cluster Active Archive: Overview, Astrophysics and Space Science Proceedings, 11, 3–37, https://doi.org/10.1007/978-90-481-3499-1_1, 2010.

Liebert, E., Nabert, C., Perschke, C., Fornaçon, K.-H., and Glassmeier, K.-H.: Statistical survey of day-side magnetospheric current flow using Cluster observations: magnetopause, Annales Geophysicae, 35, 645–657, https://doi.org/10.5194/angeo-35-645-2017, 2017.

Lopez, R. E., Merkin, V. G., and Lyon, J. G.: The role of the bow shock in solar wind-magnetosphere coupling, Annales Geophysicae, 29, 1129–1135, https://doi.org/10.5194/angeo-29-1129-2011, 2011.

Nabert, C., Glassmeier, K.-H., and Plaschke, F.: A new method for solving the MHD equations in the magnetosheath, Annales Geophysicae, 31, 419–437, https://doi.org/10.5194/angeo-31-419-2013, 2013.

Narita, Y.: Low frequency waves upstream and downstream of the terrestrial bow shock, Copernicus GmbH, Katlenburg-Lindau, 2006.

Rème, H., Bosqued, J. M., Sauvaud, J. A., Cros, A., Dandouras, J., Aoustin, C., Bouyssou, J., Camus, T., Cuvilo, J., Martz, C., Medale, J. L., Perrier, H., Romefort, D., Rouzaud, J., D'Uston, C., Mobius, E., Crocker, K., Granoff, M., Kistler, L. M., Popecki, M., Hovestadt, D., Klecker, B., Paschmann, G., Scholer, M., Carlson, C. W., Curtis, D. W., Lin, R. P., McFadden, J. P., Formisano, V., Amata, E., Bavassano-Cattaneo, M. B., Baldetti, P., Belluci, G., Bruno, R., Chionchio, G., di Lellis, A., Shelley, E. G., Ghielmetti, A. G., Lennartsson, W., Korth, A., Rosenbauer, H., Lundin, R., Olsen, S., Parks, G. K., McCarthy, M., and Balsiger, H.: The Cluster Ion Spectrometry (cis) Experiment, Space Science Reviews, 79, 303–350, https://doi.org/10.1023/A:1004929816409, 1997.

Tang, B. B., Wang, C., and Guo, X. C.: Bow shock and magnetopause contributions to the magnetospheric current system: Hints from the Cluster observations, Journal of Geophysical Research (Space Physics), 117, A01214, https://doi.org/10.1029/2011JA016681, 2012.